Bending Response of Lattice Structure Filled Tubes under Transverse Loading

Erhan Cetin 🔘   **Cengiz Baykasoğlu** 🔘
Hitit University, Department of Mechanical Engineering, Corum, Turkey

ABSTRACT

Thin-walled tubes are widely used as passive energy-absorbing structures in a variety of industries. These structures are typically filled with lightweight materials to improve their energy absorption capabilities. At this point, additive manufacturing technology offers a great chance researchers for the production of novel filler structures to increase the crashworthiness performance of thin-walled tubes. In the current work, additive manufacturable body-centered cubic (BCC) lattice structures are suggested as filling materials for thin-walled tubes, and the bending response of these structures is investigated under transverse loads via a finite element modeling approach. The aspect ratio and strut diameter are considered as design parameters, and three-point bending simulations are conducted to understand the transverse load bearing behaviors of the structures. Different loading offsets are also taken into account for three-point bending simulations. The numerical results revealed that the BCC lattice structures used as filler materials significantly increase the energy absorption performance of thin-walled tubes due to synergetic interactions. In particular, the simulation results revealed that the hybrid tubes can absorb up to 84% more energy than the empty tubes, while the crush force efficiency of these structures is up to 42% higher compared to the empty tubes. The present study also showed that the transverse crushing characteristics of tubes can be considerably improved by suitable selection of the design parameters. These primary outcomes reveal that the proposed lattice structures can be considered as a potential alternative to traditional filler materials for enhancing the bending response of thin-walled tubes under transverse loading.

Keywords:

Lattice structures; Thin-walled tubes; Energy absorption performance; Finite element methods; Transverse loading

INTRODUCTION

Thin-walled metallic tubes have been extensively used in many engineering fields as energy absorbers due to their excellent energy absorption capacities as well as their low cost [1,2]. Due to these features, the energy absorption performance of the tubes attracts the attention of researchers, and hence there are numerous analytical, numerical and experimental works have been carried out to improve the crashworthiness performances of the tubes. Different materials, geometric patterns, cross-sectional shapes and semi-apical angles are suggested in literature [2–8]. The studies reveal that the thin-walled tubes are quite successful for energy absorption applications under various load conditions including axial [9–13], oblique [14–16], lateral [17] and transverse bending [18] loads.

In recent decades, researchers have proposed low-density materials including foams [19–23], honeycombs [24,25] and composites [26–28] as filler/covering materials to enhance the crashworthiness performances of the thin-walled structures. These studies revealed that a minor increase in structural mass can significantly improve the tubes' energy absorption capabilities by using suitable filler or covering materials [5,29].

Along with the developing production technology, additive manufacturing technology enables researchers to produce complex geometries with ease. In the literature, several forms of lattice structures have been proposed, including face-centered cubic (FCC), diamond, rhombic, gyroid, body-centered cubic (BCC) and body-centered cubic with a vertical strut (BCC-Z) [30,31]. The studies reveal that low-density lattice structures as filling materials can significantly enhance the energy absorption performance of tubes without causing a significant increase in the peak crushing force of the structure. Among these structures, BCC lattice

structures stand out as the most preferred structures due to their simplicity and energy absorption performance. Herein, the energy absorption capacity, deformation behavior and mechanical properties of proposed BCC lattice structures are explored in depth in Refs. [32-40]. The corresponding studies are summarized as follows. Maskery et al. [32] investigated the influence of the cell numbers and cell size on the mechanical characteristics of BCC lattice structures subjected to tensile load. Gümrük and Mines [33] used various approaches to examine the compression behavior of BCC structures. Turner et al. [34], Shen et al. [35], Mines et al. [36] conducted research on the impact response of sandwich structures having BCC lattice structures. Gümrük et al. [37] examined the mechanical behaviors of lattice structures for BCC structures under static tensile and compressive conditions. McKown et al. [38] examined the mechanical characteristic of BCC lattice cells under both blast and quasi-static loads. In another work, in order to estimate the compressive response of BCC lattice materials, Smith et al. [39] supposed numerical models. Merkt et al. [40] investigated the mechanical response of BCC lattice materials subjected to dynamic and quasi-static loadings.

With a similar motivation, we already proposed novel BCC lattice materials as filler structures for thin-walled structures under axial and oblique loadings for the first time in the literature [41–43]. These pioneering studies revealed that the crashworthiness performance of the thin-walled tubes is remarkably enhanced by lattice structures due to the synergistic interactions. On the other hand, although the thin-walled structures are subjected to transverse loading as well as axial and oblique loads, as far as we know, no study has been studied on the energy absorption of the lattice structures filled thin-walled tubes under transverse loading. To this motivation, in the present study, the crashworthiness of thin-walled tubes improved by BCC lattice materials is investigated under transverse loads. The aspect ratio and strut diameter of the lattice structures are used as design parameters, and the hybrid structures are examined under various bending scenarios via the finite element modelling approach. At this point, five different aspect ratios, five different lattice strut diameters and five different loading scenarios are considered, and these structures are investigated by considering various crashworthiness performance criteria.

MATERIALS AND METHODS

Crashworthiness Indices

Several crashworthiness indices are used to evaluate the energy absorption performance of the energy absorber tubes under lateral loading. These indices are the total energy absorption (EA), specific energy absorption (SEA), mean crush force (MCF), peak crush force (PCF) and crush force efficiency (CFE). The EA is the total energy

absorption during the crushing period, and is calculated as follows:

$$EA = \int_0^\delta F(\delta)d\delta \tag{1}$$

where δ refers to instantaneous crushing force value throughout the effective displacement (δ). The SEA is defined as the amount of total energy absorption per unit mass, and is given as follows:

$$SEA = \frac{EA}{m} \tag{2}$$

where m is the total mass of the structure. The MCF is the ratio of total energy absorption to effective crushing displacement and is calculated as follows:

$$MCF = \frac{EA}{\delta} \tag{3}$$

The higher EA, SEA and MCF refer to better crashworthiness performance of the absorber structures [44,45]. The PCF is the maximum crushing force during the crushing period, and the high peak crushing force values may cause death or severe injury to occupants due to high deceleration. The CFE refers to the ratio of mean crush force to peak crushing force, and is calculated as follows:

$$CFE = \frac{MCF}{PCF} \tag{4}$$

It is should be noted that when the CFE value approaches unity, the deceleration will be minimized, and this is also desirable for energy absorbing structures [46].

Design Parameters

In this study, the body-centered cubic (BCC) lattice material are proposed as lightweight filler structures to enhance the crashworthiness performance of thin-walled square tubes under quasi-static lateral loadings. The aspect ratio and strut diameter are selected as design parameters. Five different aspect ratios and strut diameters of lattice structures are considered in this study. On the other hand, the tube thickness (t) and length of the structures (L) are considered as design constants and are chosen as 1.5 mm and 240 mm, respectively. The corners of the proposed lattice structures are trimmed to fit inside to tubes similar to Ref. [47]. Besides, the struts of lattice structures are designed to have an ideal geometry, which is perfectly straight. Besides, a series of bending loading conditions, namely five different offset loading for three-point bending simulations (i.e., 0, 10, 20, 30 and 40 mm) are taken into account to investigate the crashworthiness of the hybrid tubes. The proposed filler lattice structure design parameters are given in Table 1. It is should be noted that the dimensions of the proposed lattice structures vary depending on the number of lattice unit cells (i.e.,

aspect ratio) because of their cubic forms. For instance, the widths of the lattice structures having 15, 12, 10, 8 and 6-unit lattice cells are 16, 20, 24, 30 and 40mm, respectively. The hybrid tubes having several aspect ratios (i.e., L/w) are illustrated in Fig. 1, where L and w are the length and width of the structures, respectively.

Table 1. The lattice structure design parameters

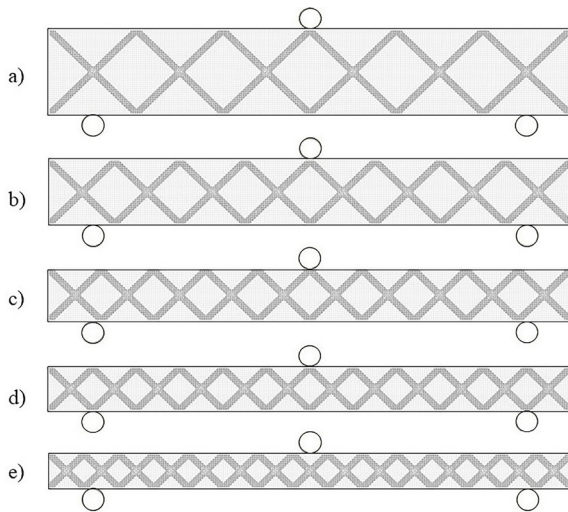| Parameters	Case 1	Case 2	Case 3	Case 4	Case 5
Aspect ratio, L/w	6	8	10	12	15
Strut diameter of lattice structure (mm), d	1	2	3	4	5

Figure 1. The representative view of hybrid structures having different filler lattice configurations a) 6 cells (L/w = 6), b) 8 cells (L/w = 8), c) 10 cells (L/w =10), d) 12 cells (L/w = 12) and e) 15 cells (L/w = 15)

Finite Element (FE) Models and Their Validation

A commercial software, SolidWorks, is used to create the geometric lattice models, and then the lattice structures are imported into the finite element software ABAQUS for the simulations. First, the hybrid structures are obtained by placing the proposed lattice structures inside thin-walled square tubes. Then, as shown in Fig. 2, three-point bending conditions are created by positioning the hybrid tube between two rigid cylindrical supports with a 200 mm-support distance (S). A movable rigid cylindrical mandrel having a prescribed velocity in the transverse direction is also situated from the top. It should be noted that the diameters of the supports and mandrel are equal to each other and are 10 mm, and the mandrel is positioned by considering the desired loading offsets (p).

4-node tetrahedral C3D4 solid elements, 4-node reduced integration S4R shell elements and 4-node linear quadrilateral R3D4 rigid elements are respectively used in the modeling of the lattice structures, thin-walled tubes and rigid structures. A mesh sensitivity analysis is carried out to
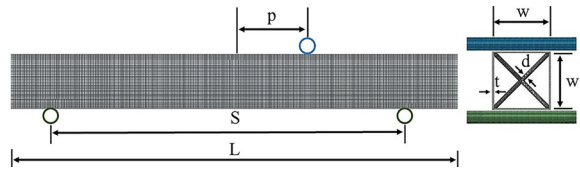

Figure 2. The schematic view of the proposed FE model of the hybrid structures under transverse loading.

provide a rational mesh size in the proposed FE model. As a result of the mesh sensitivity analyses, the mesh sizes for the tube and lattice structures are obtained as 1 mm and 2 mm, respectively. Besides, at least 3 elements are employed throughout the diameters of the lattice structures similar to Ref. [48]. The interaction between the hybrid tubes and rigid structures is introduced by the general contact formulation and the friction coefficient is considered as 0.3 for all contact situations [49]. The material of the tube, Al6063-T5, has yield strength of 187 MPa, Young's modulus of 68.2 GPa, Poisson ratio of 0.33 and density of 2700 kg/m3 [50]. On the other hand, the material of the lattice structure, AlSi10Mg, has yield strength of 160 MPa, Young's modulus of 69.3 GPa, Poisson ratio of 0.3 and density of 2670 kg/m3 [51]. The von Mises yield criteria is used to define isotropic yielding. It is should be noted that the 6-series aluminum alloys generally show low strain-rate sensitivity, thus, the strain rate effect is not considered in the FE analysis, similar to literature [52,53].
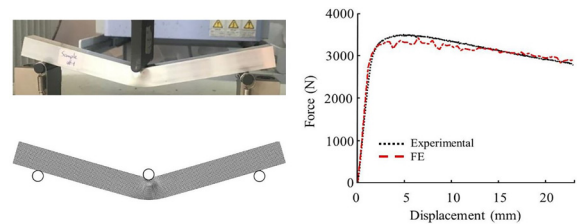

Figure 3. Comparison of deformation shapes and force-displacement curves obtained from experimental test and FE simulation.

In our previous studies [41–43], the numerical model are already validated by considering different loading condition (i.e., axial and oblique loads) by comparing the predicted force-displacement responses and deformation modes with the experimental results. In this study, the transverse loading case is also taken into account as a scenario to further strengthen the model validation. At this point, the quasi-static experimental tests are executed at a constant crosshead speed of 0.5 mm/s [49], using Shimadzu universal testing machine with a load cell of 100 kN. Al6063-T5 thin-walled square tubes with a length of 250 mm, cross-sectional area of 20x20 mm² and 1.5 mm tube thickness are used for validation tests. At least three quasi-static bending tests are performed to check the consistency of the experimental results. The bending deformation process is captured by a high-resolution digital camera. The three-point bending test set-up is shown in Fig. 3. It is should be noted that

Table 2. Comparison of crashworthiness performances of empty and hybrid tubes

Structure Type	Aspect ratio (L/w)	Lattice strut diameter (d) (mm)	Mass (g)	Loading Offset (p)(mm)	EA (J)	SEA (J/g)	MCF (kN)	PCF (kN	CFE
Tube	10	-	99.10	0	183.28	1.85	3.67	7.65	0.48
				20	188.26	1.90	3.77	7.74	0.49
				40	202.70	2.05	4.06	7.67	0.53
Hybrid	10	5	170.70	0	318.54	1.87	6.37	10.27	0.62
				20	319.67	1.87	6.39	11.15	0.57
				40	330.58	1.94	6.61	8.85	0.75
Tube	12	-	83.60	0	154.47	1.85	3.09	6.80	0.45
				20	160.50	1.92	3.22	6.94	0.46
				40	175.72	2.10	3.52	6.83	0.52
Hybrid	12	5	151.90	0	275.53	1.81	5.52	10.01	0.55
				20	285.87	1.88	5.73	9.93	0.58
				40	323.90	2.13	6.48	9.17	0.71

that the quasi-static simulations can be carried out by using various methods such as mass and/or velocity scaling approaches. In the present work, the FE simulations are executed via Abaqus/Explicit code using a scale-up method, similar to Refs. [54–56], in order to achieve the optimal balance between computing efficiency and accuracy. At this point, a ramp profile is defined to reduce the inertial effect, and then, at a constant speed of 2 m/s, the FE simulations are run. To use this approach, the force-displacement curve must be independent of loading velocities, and the ratio of total kinetic energy to total internal energy must be less than 5% throughout the crushing process. The force-displacement curves obtained by experimental measurement and FE simulation are also compared in Fig. 3. The results show that the maximum difference between the experimental and FE results is approximately 2%, which means that the results from the proposed FE model are quite reliable.

RESULTS AND DISCUSSION

In this section, firstly, the energy absorption performances of hybrid designs are compared with empty tubes in order to reveal the contribution of synergistic effects to the improvement of the energy absorption capacity at the same volume. Then, the effects of strut diameter and aspect ratio on the bending responses of hybrid tubes are examined by considering different offset loading conditions. In Table 2, the bending responses of the empty tube and hybrid tube having different aspect ratios are compared by considering different loading conditions.

It is clearly seen from the table that when a lattice structure is placed in the thin-walled tube, the EA increases as expected. However, the low-density lattice structures as filler material can significantly improve the energy absorption performance of the square tubes without increasing the volume of the structures. For instance, although the SEA values of the empty and hybrid tubes with an aspect ratio of 10

are similar, the hybrid tube has 74% higher EA values than that of the empty tube for central loading. Similarly, the EA value of the hybrid structure having an aspect ratio of 12 is about 84% higher than that of the empty tube for a 40 mm loading offset. On the other hand, since the proposed lattice structures are lightweight materials with low density, the PCF values of the structures do not increase much. At this point, when the CFE which is a parameter that determines the correlation between MCF and PCF, is examined, it is seen that the CFE value of the hybrid tube with an aspect ratio of 10 is approximately 42% higher than that of the empty tube. The results reveal that the crushing performances of the empty tubes can be remarkably improved with the suggested lattice structures under transverse loading owing to synergetic interactions between lattice structures and tubes.
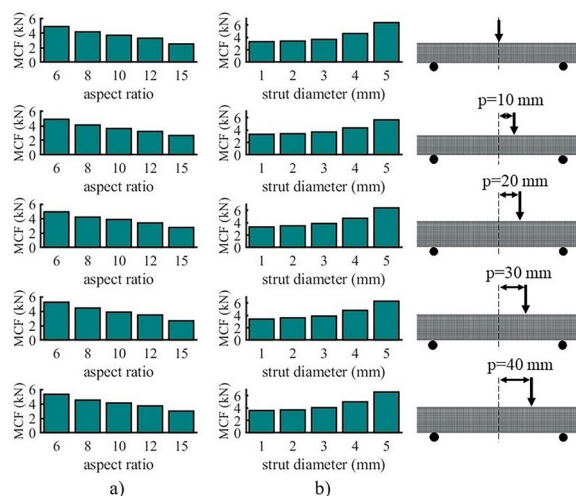

Figure 4. The MCF values of hybrid tubes having different a) aspect ratios and b) strut diameters of lattice element for different offset loading positions.

The MCF values of the hybrid tubes having 3 mm strut diameter and different aspect ratios are given in Fig. 4a for different offset loading conditions. As the aspect ratio of

the hybrid tubes increases, the cross-sectional areas of the structures and accordingly load-carrying capacities decrease. Hence, the MCF values of the hybrid tubes decrease in all cases as the aspect ratio increases. For instance, the MCF value of the 6-cell hybrid tube is about 99.2% higher than that of the 15-cell for central loading condition. On the other hand, the MCF values of the hybrid tubes with different lattice strut diameters are shown in Fig. 4b for the aspect ratio of 10. As seen in the figure, the MCF values increase as the increasing strut diameter. However, a remarkable improvement in MCF values can be achieved for strut diameter values above 3 mm. In particular, for the 10-cell design, the MCF value of the hybrid structure with a strut diameter of 5 mm is about 94 % higher than that of a hybrid structure with a strut diameter of 1 mm. Besides, as shown in the figure, the MCF values of the hybrid tubes slightly increase as the mandrel is positioned away from the center. At this point, the MCF value of the hybrid tube under bending loading with an offset position of 40 mm is up to 24.2% higher than that of the center loading condition.
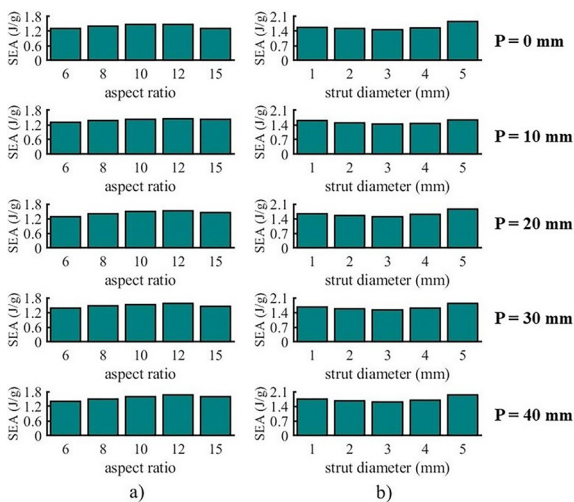
of 1-3 mm while the SEA values relatively increase as the strut diameter increase for strut diameter greater than 3 mm. For example, the SEA value of the hybrid structure with a strut diameter of 5 mm is approximately 17% higher than that of a 3mm-hybrid structure for central loading. Similar values are observed for other loading offsets.

The CFE values of the hybrid tubes having a strut diameter of 3 mm and different aspect ratios are shown in Fig. 6a for different offset loading positions. It is seen that the CFE values for all loading conditions are around 0.5 and the aspect ratios have no significant effect on the CFE values of the tubes. On the other hand, the CFE values of 10-cell hybrid tubes with different strut diameters under transverse loading are shown in Fig. 6b. As seen in the figure, CFE values increase as the diameter value increases for the same loading condition. In particular, for the central loading, the CFE value of the hybrid structure with a strut diameter of 5 mm is approximately 67.6% higher than that of the hybrid structure with a strut diameter of 1 mm. The reason for this can be explained as the fact that although the PCF values of the hybrid tubes are similar to each other, the MCF values with a 5 mm strut diameter are higher than the others. Similarly, this case is also valid for different loading offsets. For example, the CFE value of the hybrid structure having a strut diameter of 5 mm is approximately 56.3% higher than that of the hybrid structure with a strut diameter of 1 mm, for the 40 mm loading offset.
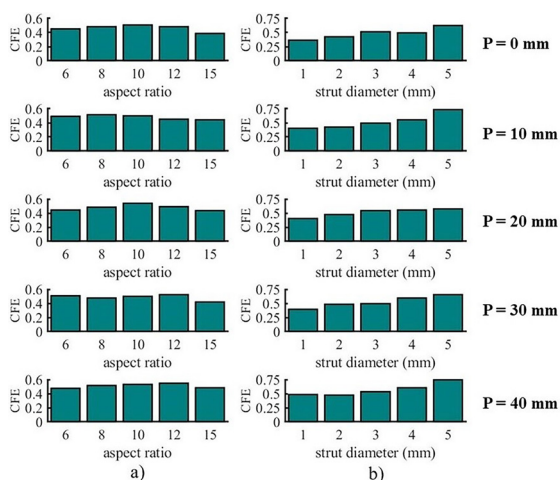

Figure 5. The SEA values of hybrid tubes having different a) aspect ratios and b) strut diameters of lattice element for different offset loading positions

The SEA values of the hybrid tubes with a strut diameter of 3 mm and different aspect ratios are shown in Fig. 5a for different offset loading positions. It can be observed from the figure that there is a slight increase in the SEA values of the hybrid tubes as the aspect ratio increases. At this point, the 12-cell hybrid structures have the highest SEA performance since the intersection areas of the lattice structure in the hybrid design are close to the support which lead to extra rigidity. Furthermore, when the hybrid tubes having the same aspect ratios are considered, no significant increase is observed in SEA values among the different loading conditions. On the other hand, the SEA values of the hybrid tubes having different strut diameters are given in Fig. 5b for an aspect ratio of 10. As shown in the figure, the SEA values of the hybrid tubes are similar for the strut diameter range

Figure 6. The CFE values of hybrid tubes having different a) aspect ratios and b) strut diameters of lattice element for different offset loading positions

There are various deformation modes such as indentation, bending with indentation and bending collapse modes for hybrid tubes under bending load in the literature. These modes can be seen in the collapse of empty [57,58], foam-filled [59], tube-filled [60] and embedded multi-cell [61] tubes for three-point bending. The illust-
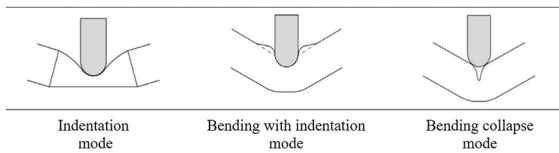
Figure 7. The illustration for indentation, bending with indentation and bending collapse modes under three-point bending [57].

ration and final deformation views of the hybrid tubes for transverse loading conditions are shown in Fig. 7 and Fig. 8, respectively. As can be observed from the figures, the indentation mode of the tubes is generated by the higher resistance, which delays the formation of the inward fold compared to the bending collapse mode [59,61]. Besides, the aspect ratios have a dominant effect on the deformation modes of the hybrid tubes. It is observed that there is a transition from indentation mode to bending mode as the aspect ratio increase. For example, the indentation mode is dominant in the 6-cell hybrid structure while the bending mode is dominant in the 15-cell structure.
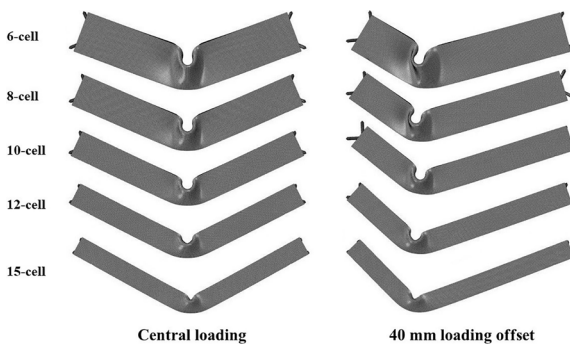

Figure 8. Final bending view of hybrid structures having different aspect ratios for central loading and 40 mm loading offset.

CONCLUSION

In this work, the bending response of thin-walled tubes filled with body-centered cubic (BCC) lattice materials is investigated under transverse loads via finite element modeling approach. As design parameters, the aspect ratio and strut diameter are chosen for hybrid tube configurations, and various transverse loading scenarios are used for bending simulations. At this point, five different aspect ratios, five different strut diameters and five different loading offsets are considered in the present study. The numerical results showed that the hybrid tubes could absorb up to 84% more crushing energy compared to the empty tube while the CFE value of the hybrid tubes is 42 % higher than that of the empty tube due to synergetic interactions between lattice structures and tubes. Besides, it is seen that as the aspect ratio increases, the MCF values of the hybrid tubes decrease for all proposed designs. In particular, the MCF of the 6-cell hybrid tube is found to be approximately 99.2% higher than the MCF of the 15-cell tube for central loading conditions. In addition, it is seen that the proposed structures have more effective

when the strut diameter values of the lattice structures placed in the tube are higher than 3 mm. This study also revealed that the bending deformation behavior of the tubes can be enhanced with the proper selection of the lattice design parameters. The main findings show that the proposed lattice structures could be used instead of traditional filler structures to enhance the energy absorption capacity of thin-walled tubes under transverse loading. Further studies will focus on other various filler lattice topologies (e.g., face-centered cubic, gyroid) unlike the BCC lattice structures proposed in this study. In addition, further studies will also be investigated the crashworthiness performances of the functionally graded lattice structures with variable stiffness for the filler materials of the tubes.

CONFLICT OF INTEREST

Authors approve that to the best of their knowledge, there is not any conflict of interest or common interest with an institution/organization or a person that may affect the review process of the paper.

AUTHOR CONTRIBUTION

All the work in this study were performed equally by the authors.

REFERENCES

1. Meran AP, Baykasoglu C, Mugan A. Development of a design for a crash energy management system for use in a railway passenger car. Proc Inst Mech Eng Part F J Rail Rapid Transit 2016;230:206–19. https://doi.org/10.1177/0954409714533321.

2. Bhutada S, Goel MD. Crashworthiness parameters and their improvement using tubes as an energy absorbing structure: an overview. Int J Crashworthiness 2021;0:1–32. https://doi.org/10.1080/13588265.2021.1969845.

3. Abramowicz W. Thin-walled structures as impact energy absorbers. Thin-Walled Struct 2003;41:91–107. https://doi.org/10.1016/S0263-8231(02)00082-4.

4. Alghamdi AAA. Collapsible impact energy absorbers: An overview. Thin-Walled Struct 2001;39:189–213. https://doi.org/10.1016/S0263-8231(00)00048-3.

5. Baroutaji A, Sajjia M, Olabi AG. On the crashworthiness performance of thin-walled energy absorbers: Recent advances and future developments. Thin-Walled Struct 2017;118:137–63. https://doi.org/10.1016/j.tws.2017.05.018.

6. Mat F, Ismail KA, Yaacob S, Inayatullah O. Impact Response of Thin-Walled Tubes: A Prospective Review. Appl Mech Mater 2012;165:130–4. https://doi.org/10.4028/www.scientific.net/AMM.165.130.

7. Olabi AG, Morris E, Hashmi MSJ. Metallic tube type energy absorbers: A synopsis. Thin-Walled Struct 2007;45:706–26. https://doi.org/10.1016/j.tws.2007.05.003.

8. Yuen SCK, Nurick GN. The Energy-Absorbing Characteristics of Tubular Structures With Geometric and Material Modifications: An Overview. Appl Mech Rev 2008;61:020802. https://doi.org/10.1115/1.2885138.

9. Karagiozova D, Alves M. Transition from progressive buckling to global bending of circular shells under axial impact - Part I: Experimental and numerical observations. Int J Solids Struct 2004;41:1565–80. https://doi.org/10.1016/j.ijsolstr.2003.10.005.

10. Karagiozova D, Jones N. Dynamic effects on buckling and energy absorption of cylindrical shells under axial impact. Thin-Walled Struct 2001;39:583–610. https://doi.org/10.1016/S0263-8231(01)00015-5.

11. Baykasoglu C, Cetin MT. Energy absorption of circular aluminium tubes with functionally graded thickness under axial impact loading. Int J Crashworthiness 2015;20:95–106. https://doi.org/10.1080/13588265.2014.982269.

12. Emin M, Baykasoglu C, Tunay M. Quasi-static Axial Crushing Behavior of Thin-walled Circular Aluminum Tubes with Functionally Graded Thickness. Procedia Eng 2016;149:559–65. https://doi.org/10.1016/j.proeng.2016.06.705.

13. Baykasoglu A, Baykasoglu C. Crashworthiness optimization of circular tubes with functionally-graded thickness. Eng Comput 2016;33:1560–85. https://doi.org/10.1108/EC-08-2015-0245.

14. Qi C, Yang S. Crashworthiness and lightweight optimisation of thin-walled conical tubes subjectedto an oblique impact. Int J Crashworthiness 2014;19:334–51. https://doi.org/10.1080/13588265.2014.893788.

15. Yang S, Qi C. Multiobjective optimization for empty and foam-filled square columns under oblique impact loading. Int J Impact Eng 2013;54:177–91. https://doi.org/10.1016/j.ijimpeng.2012.11.009.

16. Baykasoğlu C, Baykasoğlu A, Tunay Çetin M. A comparative study on crashworthiness of thin-walled tubes with functionally graded thickness under oblique impact loadings. Int J Crashworthiness 2019;24:453–71. https://doi.org/10.1080/13588265.2018.1478775.

17. Qiu N, Gao Y, Fang J, Sun G, Kim NH. Topological design of multi-cell hexagonal tubes under axial and lateral loading cases using a modified particle swarm algorithm. Appl Math Model 2018;53:567–83. https://doi.org/10.1016/j.apm.2017.08.017.

18. Huang Z, Zhang X, Fu X. On the bending force response of thin-walled beams under transverse loading. Thin-Walled Struct 2020;154:106807. https://doi.org/10.1016/j.tws.2020.106807.

19. Gao Q, Wang L, Wang Y, Guo F, Zhang Z. Optimization of foam-filled double ellipse tubes under multiple loading cases. Adv Eng Softw 2016;99:27–35. https://doi.org/10.1016/j.advengsoft.2016.05.001.

20. Yu X, Qin Q, Zhang J, Wang M, Xiang C, Wang T. Low-velocity impact of density-graded foam-filled square columns. Int J Crashworthiness 2020;0:1–14. https://doi.org/10.1080/13588265.2020.1807685.

21. Altin M, Güler MA, Mert SK. The effect of percent foam fill ratio on the energy absorption capacity of axially compressed thin-walled multi-cell square and circular tubes. Int J Mech Sci 2017;131–132:368–79. https://doi.org/10.1016/j.ijmecsci.2017.07.003.

22. Altin M, Acar E, Güler MA. Foam filling options for crashworthiness optimization of thin-walled multi-tubular circular columns. Thin-Walled Struct 2018;131:309–23. https://doi.org/10.1016/j.tws.2018.06.043.

23. Gedikli H. Crashworthiness optimization of foam-filled tailor-welded tube using coupled finite element and smooth particle hydrodynamics method. Thin-Walled Struct 2013;67:34–48. https://doi.org/10.1016/j.tws.2013.01.020.

24. Fang J, Sun G, Qiu N, Pang T, Li S, Li Q. On hierarchical honeycombs under out-of-plane crushing. Int J Solids Struct 2018;135:1–13. https://doi.org/10.1016/j.ijsolstr.2017.08.013.

25. Zhu G, Li S, Sun G, Li G, Li Q. On design of graded honeycomb filler and tubal wall thickness for multiple load cases. Thin-Walled Struct 2016;109:377–89. https://doi.org/10.1016/j.tws.2016.09.017.

26. Song HW, Wan ZM, Xie ZM, Du XW. Axial impact behavior and energy absorption efficiency of composite wrapped metal tubes. Int J Impact Eng 2000;24:385–401. https://doi.org/10.1016/S0734-743X(99)00165-7.

27. Zhu G, Sun G, Liu Q, Li G, Li Q. On crushing characteristics of different configurations of metal-composites hybrid tubes. Compos Struct 2017;175:58–69. https://doi.org/10.1016/j.compstruct.2017.04.072.

28. Meriç D, Gedikli H. Multi-objective optimization of energy absorbing behavior of foam-filled hybrid composite tubes. Compos Struct 2022;279:114771. https://doi.org/10.1016/j.compstruct.2021.114771.

29. Sun G, Chen D, Zhu G, Li Q. Lightweight hybrid materials and structures for energy absorption: A state-of-the-art review and outlook. Thin-Walled Struct 2022;172:108760. https://doi.org/10.1016/j.tws.2021.108760.

30. Mahmoud D, Elbestawi MA. Lattice structures and functionally graded materials applications in additive manufacturing of orthopedic implants: A review. J Manuf Mater Process 2017;1:1–19. https://doi.org/10.3390/jmmp1020013.

31. Pan C, Han Y, Lu J. Design and optimization of lattice structures: A review. Appl Sci 2020;10:1–36. https://doi.org/10.3390/APP10186374.

32. Maskery I, Aremu AO, Simonelli M, Tuck C, Wildman RD, Ashcroft IA, et al. Mechanical Properties of Ti-6Al-4V Selectively Laser Melted Parts with Body-Centred-Cubic Lattices of Varying cell size. Exp Mech 2015:1–12. https://doi.org/10.1007/s11340-015-0021-5.

33. Gümrük R, Mines RAW. Compressive behaviour of stainless steel micro-lattice structures. Int J Mech Sci 2013;68:125–39. https://doi.org/10.1016/j.ijmecsci.2013.01.006.

34. Turner AJ, Al Rifaie M, Mian A, Srinivasan R. Low-Velocity Impact Behavior of Sandwich Structures with Additively Manufactured Polymer Lattice Cores. J Mater Eng Perform 2018;27:2505–12. https://doi.org/10.1007/s11665-018-3322-x.

35. Shen Y, Cantwell W, Mines R, Li Y. Low-velocity impact performance of lattice structure core based sandwich panels. J Compos Mater 2014;48:3153–67. https://doi.org/10.1177/0021998313507616.

36. Mines RAW, Tsopanos S, Shen Y, Hasan R, McKown ST. Drop weight impact behaviour of sandwich panels with metallic micro lattice cores. Int J Impact Eng 2013;60:120–32. https://doi.org/10.1016/j.ijimpeng.2013.04.007.

37. Gümrük R, Mines RAW, Karadeniz S. Static mechanical behaviours of stainless steel micro-lattice structures under different loading conditions. Mater Sci Eng A 2013;586:392–406. https://doi.org/10.1016/j.msea.2013.07.070.

38. McKown S, Shen Y, Brookes WK, Sutcliffe CJ, Cantwell WJ, Langdon GS, et al. The quasi-static and blast loading response of lattice structures. Int J Impact Eng 2008;35:795–810. https://doi.org/10.1016/j.ijimpeng.2007.10.005.

39. Smith M, Guan Z, Cantwell W. J. Finite element modelling of the compressive response of lattice structures manufactured using the selective laser melting technique. Int J Mech Sci 2013;67:28–41. https://doi.org/10.1016/j.ijmecsci.2012.12.004.

40. Merkt S, Hinke C, Bültmann J, Brandt M, Xie YM. Mechanical response of TiAl6V4 lattice structures manufactured by selective laser melting in quasistatic and dynamic compression tests. J Laser Appl 2015;27:S17006. https://doi.org/10.2351/1.4898835.

41. Cetin E, Baykasoğlu C. Energy absorption of thin-walled tubes enhanced by lattice structures. Int J Mech Sci 2019;158:471–84. https://doi.org/10.1016/j.ijmecsci.2019.04.049.

42. Baykasoğlu A, Baykasoğlu C, Cetin E. Multi-objective crashworthiness optimization of lattice structure filled thin-walled tubes. Thin Walled Struct 2020;149. https://doi.org/10.1016/j.tws.2020.106630.

43. Cetin E, Baykasoğlu C. Crashworthiness of graded lattice structure filled thin-walled tubes under multiple impact loadings. Thin-Walled Struct 2020;154. https://doi.org/10.1016/j.tws.2020.106849.

44. Gao Q, Wang L, Wang Y, Wang C. Crushing analysis and multiobjective crashworthiness optimization of foam-filled ellipse tubes under oblique impact loading. Thin-Walled Struct 2016;100:105–12. https://doi.org/10.1016/j.tws.2015.11.020.

45. Li G, Xu F, Sun G, Li Q. A comparative study on thin-walled structures with functionally graded thickness (FGT) and tapered tubes withstanding oblique impact loading. Int J Impact Eng 2015;77:68–83. https://doi.org/10.1016/j.ijimpeng.2014.11.003.

46. Qiu N, Gao Y, Fang J, Feng Z, Sun G, Li Q. Crashworthiness analysis and design of multi-cell hexagonal columns under multiple loading cases. Finite Elem Anal Des 2015;104:89–101. https://doi.org/10.1016/j.finel.2015.06.004.

47. Li P, Wang Z, Petrinic N, Siviour CR. Deformation behaviour of stainless steel microlattice structures by selective laser melting. Mater Sci Eng A 2014;614:116–21. https://doi.org/10.1016/j.msea.2014.07.015.

48. Tripathy L, Lu WF. Evaluation of axially-crushed cellular truss structures for crashworthiness. Int J Crashworthiness 2017;8265:1–17. https://doi.org/10.1080/13588265.2017.1389630.

49. Zhang X, Zhang H, Wang Z. Bending collapse of square tubes with variable thickness. Int J Mech Sci 2016;106:107–16. https://doi.org/10.1016/j.ijmecsci.2015.12.006.

50. Karagiozova D, Nurick GN, Chung Kim Yuen S. Energy absorption of aluminium alloy circular and square tubes under an axial explosive load. Thin-Walled Struct 2005;43:956–82. https://doi.org/10.1016/j.tws.2004.11.002.

51. Zhang Y, Liu T, Ren H, Maskery I, Ashcroft I. Dynamic compressive response of additively manufactured AlSi10Mg alloy hierarchical honeycomb structures. Compos Struct 2018;195:45–59. https://doi.org/10.1016/j.compstruct.2018.04.021.

52. Zheng G, Wu S, Sun G, Li G, Li Q. Crushing analysis of foam-filled single and bitubal polygonal thin-walled tubes. Int J Mech Sci 2014;87:226–40. https://doi.org/10.1016/j.ijmecsci.2014.06.002.

53. Bai Z, Sun K, Zhu F, Cao L, Hu J, Chou CC, et al. Crashworthiness optimal design of a new extruded octagonal multi-cell tube under dynamic axial impact. Int J Veh Saf 2018;10:40–57. https://doi.org/10.1504/IJVS.2018.093056.

54. Hu D, Wang YY, Song B, Wang YY. Energy absorption characteristics of a foam-filled tri-tube under axial quasi-static loading: experiment and numerical simulation. Int J Crashworthiness 2018;23:417–32. https://doi.org/10.1080/13588265.2017.1331494.

55. Azarakhsh S, Ghamarian A. Collapse behavior of thin-walled conical tube clamped at both ends subjected to axial and oblique loads. Thin-Walled Struct 2017;112:1–11. https://doi.org/10.1016/j.tws.2016.11.020.

56. Zhu G, Sun G, Li G, Cheng A, Li Q. Modeling for CFRP structures subjected to quasi-static crushing. Compos Struct 2018;184:41–55. https://doi.org/10.1016/j.compstruct.2017.09.001.

57. Huang Z, Zhang X. Three-point bending collapse of thin-walled rectangular beams. Int J Mech Sci 2018;144:461–79. https://doi.org/10.1016/j.ijmecsci.2018.06.001.

58. Huang Z, Zhang X. Three-point bending of thin-walled rectangular section tubes with indentation mode. Thin-Walled Struct 2019;137:231–50. https://doi.org/10.1016/j.tws.2019.01.015.

59. Santosa S, Banhart J, Wierzbicki T. Experimental and numerical analyses of bending of foam-filled sections. Acta Mech 2001;148:199–213. https://doi.org/10.1007/BF01183678.

60. Zhang X, Zhang H. Static and dynamic bending collapse of thin-walled square beams with tube filler. Int J Impact Eng 2018;112:165–79. https://doi.org/10.1016/j.ijimpeng.2017.11.001.

61. Zhang X, Zhang H, Leng K. Experimental and numerical investigation on bending collapse of embedded multi-cell tubes. Thin-Walled Struct 2018;127:728–40. https://doi.org/10.1016/j.tws.2018.03.011.